JOURNAL OF Materials CHEMISTRY

Structure and photoelectric properties of tetrakis(4-*N*-hexadecylpyridiniumyl)porphyrin/anthraquinone LB films

Xuezhong He,*[a] Yuxiang Zhou,[a] Yalin Zhou,[b] Lingxuan Wang,[b] Tiankai Li,[b] Zhichu Bi,[b] Manhua Zhang[b] and Tao Shen[b]

[a]*Department of Biological Science and Biotechnology, Tsinghua University, Beijing 100084, P.R. China. E-mail: hexzh@263.net*
[b]*Institute of Photographic Chemistry, The Chinese Academy of Science, Beijing 100101, P.R. China*

Received 1st October 1999, Accepted 17th December 1999

Using a 1 : 1 tetrakis(4-*N*-hexadecylpyridiniumyl)porphyrin/anthraquinone ($TC_{16}PyP(4)$/AnQ) mixture as film-forming material, the structure and properties of $TC_{16}PyP(4)$/AnQ mixed monolayers or LB films were studied by π–A isotherms, UV–VIS absorption spectra, and low-angle X-ray diffraction (LAXD). The experimental results indicate that the $TC_{16}PyP(4)$/AnQ mixture has good film-forming properties at the air/water interface. The $TC_{16}PyP(4)$/AnQ mixed monolayer can be transferred to glass, quartz or SnO_2 optically transparent electrode (OTE) substrates. Most AnQ molecules are incorporated into the cavities between the long alkyl chains of $TC_{16}PyP(4)$ molecules in the mixed monolayer or in LB films. The $TC_{16}PyP(4)$/AnQ mixed LB films can be regarded as a two-dimensional host–guest system and show good stability and periodicity. The photovoltaic behaviour of an electrochemical cell containing a $TC_{16}PyP(4)$/AnQ LB film, deposited on an SnO_2 OTE, was also investigated. The photocurrent and photovoltage are apparently lower than those for the photocell of pure $TC_{16}PyP(4)$ LB films due to the incorporation of AnQ.

1 Introduction

In recent years, study on the conversion and application of solar energy has been one of the most active aspects in the field of new energetic source development, with the fabrication of novel solar energy cells a predominant goal.[1,2] Inorganic semiconductive solar energy cells have been applied in the military and aerospace fields, but their high cost and complicated fabrication have hampered extensive application. Solar cells made from organic materials have received increasing interest due mainly to their low cost and ease of fabrication.[3] Such organic semiconductors have often been used for electrophotography in the form of thin film.[4] Porphyrins are thermally and chemically stable organic semiconductors and have been widely used in photovoltaic devices.[5,6] As far as film-forming materials are concerned, the use of porphyrins for such studies has two main advantages: (i) one can obtain molecules with various molecular structures and (ii) porphyrins are generally fairly insensitive to photodegradation.

We have been studying photophysical and photochemical properties of porphyrin LB films with the aim of constructing molecular electronic devices. In a previous paper[7] we studied the photovoltaic behavior of an electrochemical cell derived from tetrakis(4-*N*-hexadecylpyridiniumyl)porphyrin [$TC_{16}PyP(4)$, Fig. 1] LB films deposited on an SnO_2 optically transparent electrode (OTE) and found a photocurrent increase in the presence of electron donors or acceptors in the electrolyte solution. Xu and coworkers[8] reported that an improvement in the photovoltaic effect of a mixed thin film consisting of a porphyrin and a phthalocyanine spin-coated on a SnO_2 electrode was observed in comparison with films coated with the individual dyes. We thus inferred that new optical and photoelectric properties may be observed when a donor or acceptor molecule with appropriate size is incorporated into the cavity of the symmetrically substituted porphyrin $TC_{16}PyP(4)$ by the LB film technique.

Here, we study the film-forming properties of a 1 : 1 $TC_{16}PyP(4)$/anthraquinone (AnQ) mixture at the air/water interface by using 1 : 1 $TC_{16}PyP(4)$/AnQ as the film-forming material, and determine the structure and properties of the porphyrin/AnQ mixed LB films. AnQ was chosen because of its large π-electron system and the observed effective intramolecular photoinduced electron transfer in porphyrin–quinone systems.[9–11] The photoelectric properties of $TC_{16}PyP$/AnQ mixed LB films, deposited on SnO_2 optically transparent electrodes (SnO_2 OTE), were also investigated in bicell, bielectrode systems.

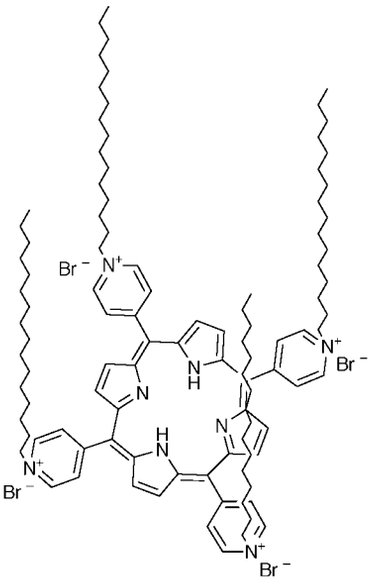

Fig. 1 Structure of $TC_{16}PyP(4)$.

DOI: 10.1039/a907900i

2 Experimental

2.1 Materials

The reagents used were all of analytical grades. The amphiphilic porphyrin $TC_{16}PyP(4)$ was prepared according to a described procedure.[12] All the samples were tested by elemental analysis and their homogeneity was checked by TLC.

2.2 Monolayer formation and LB film preparation

Monolayer formation and deposition were carried out on a Joyle–Loebel Langmuir Trough 4 at room temperature ($20 \pm 1\,^{\circ}C$). The surface pressure was measured by the Wilhelmy method.[13] Triple-distilled deionized water (pH = 5.8) was used as the subphase. The monolayer was spread on the pure water subphase from a solution of $TC_{16}PyP(4)$ or a solution of equimolar $TC_{16}PyP(4)$ and AnQ. The concentration of $TC_{16}PyP(4)$ and AnQ was 1×10^{-4} M in all these spreading solutions. After the spreading solutions were spread onto the subphase using a microsyringe, compression was started and the π–A curves were recorded 15 min later when the solvent had evaporated. All the substrates were cleaned successively with chloroform, acetone and isopropyl alcohol and finally subjected to ultrasound for 30 min before use. The LB films of $TC_{16}PyP(4)$ and $TC_{16}PyP(4)$/AnQ were deposited on quartz slides for electronic spectra, glass slides for LAXD and SnO_2 OTE for photovoltaic measurements respectively, *via* the vertical dipping method, resulting in a fairly good deposition of a typical Y-mode film with a transfer ratio of 1.02. Monolayer deposition was performed under a surface pressure of 30 mN m^{-1} unless otherwise stated, while the dipping speed was 2 mm min^{-1}.

2.3 Absorption spectra and LAXD measurements

UV–VIS absorption spectra were measured using a Shimadzu UV-160A spectrophotometer. LAXD measurements were carried out on a D/max-γ A X-ray diffractometer (Cu-Kα line radiation, $\lambda = 1.5405$ Å).

2.4 Photoelectrochemical measurements

The photocurrent and photovoltage were determined on a computer-controlled microcurrentmeter (Fig. 2). The electrochemical cell was made up of the bicell, which was linked by an agar salt bridge in order to increase the photovoltaic signal/noise ratio. The electrochemical cell thus prepared as well as all the electrical cables was shielded with an iron box against electromagnetic perturbations. A 500 W xenon arc lamp was used as the light source. Since the blank photocurrent due to SnO_2 OTE excitation had a measurable value at wavelengths below 390 nm, illumination was performed with wavelengths above 390 nm, using a cut-off filter. The photocurrent and photovoltage were measured with a homemade picoammeter and potentiostat, respectively. The photovoltaic signals were recorded on a computer for data treatment. The supporting electrolyte was 0.1 mol L^{-1} KCl aqueous solution, to which an electron donor or acceptor could be added.[14] The experimental photovoltaic cell can be represented as: SnO_2 OTE/$TC_{16}PyP(4)$/AnQ LB film/0.1 mol L^{-1} KCl aqueous solution/agar salt bridge/saturated KCl solution/SCE.

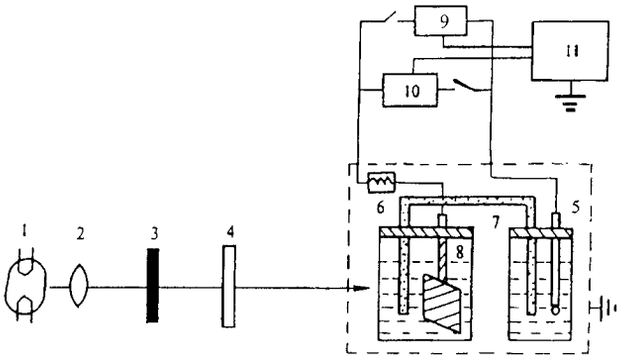

Fig. 2 Schematic diagram of the setup for the photocurrent measurement. 1, light source; 2, focusing lens; 3, shutter; 4, cut-off filter; 5, SCE; 6, resistor; 7, agar salt bridge; 8, $TC_{16}PyP(4)$/AnQ-deposited SnO_2 OTE; 9, potentiostat; 10, picoammeter; 11, computer for data retrieval.

3 Results and discussion

3.1 π–A isotherms of a pure $TC_{16}PyP(4)$ monolayer and of a $TC_{16}PyP(4)$/AnQ mixed monolayer

Fig. 3 compares the π–A isotherms of a pure $TC_{16}PyP(4)$ monolayer and a 1 : 1 $TC_{16}PyP(4)$/AnQ mixed monolayer on a pure water subphase. The solid and dashed lines in Fig. 3 indicate the π–A isotherms of pure $TC_{16}PyP(4)$ and the 1 : 1 $TC_{16}PyP(4)$/AnQ mixture, respectively. All curves were reproducible. As can be seen, both $TC_{16}PyP(4)$ and 1 : 1 $TC_{16}PyP(4)$/AnQ mixtures form stable monolayers at the air/water interface (with collapse pressure > 45 mN m^{-1}). For the pure $TC_{16}PyP(4)$ monolayer, the π–A isotherm shows a distinct phase transition and an abrupt increase in slope, with no well defined collapse being observed up to 50 mN m^{-1}, the limit of our apparatus. At a surface pressure of *ca.* 30 mN m^{-1}, the monomolecular area (extrapolating the linear part of the π–A isotherm to the abscissa) is 2.20 nm^2. In a previous paper[7] we reported that a molecular area of *ca.* 2.40 nm^2 is expected if the porphyrin ring is oriented parallel to the aqueous surface while an area of 1.10 nm^2 is expected if it is oriented perpendicular to the aqueous surface according to a Corey–Pauling–Kolturn (CPK) molecular model.[15] We thus infer that the porphyrin ring is oriented with an angle of 24° to the aqueous surface. For the 1 : 1 mixture of $TC_{16}PyP(4)$/AnQ, the collapse pressure is 45 mN m^{-1}. The apparent monomolecular area at 30 mN m^{-1} (extrapolating the solid film part of the π–A isotherm to the abscissa) is 2.10 nm^2 (area calculations are based on the concentration of porphyrin molecules).

For most mixed monolayers, the apparent monomolecular area obtained from π–A isotherms should be greater than that of each component. However, the monomolecular area of the $TC_{16}PyP(4)$/AnQ mixture is slightly smaller than that of $TC_{16}PyP(4)$. This indicates that anthraquinone molecules do not occupy the space between porphyrin molecules in mixed monolayers. This is similar to Yang's result[16] that the

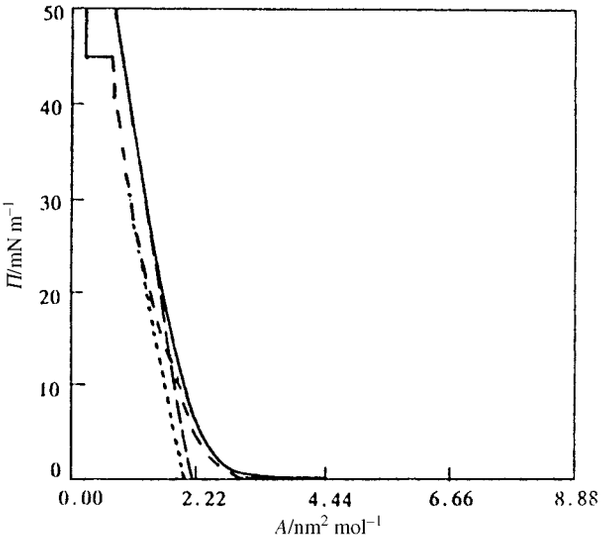

Fig. 3 π–A isotherms of a pure $TC_{16}PyP(4)$ monolayer (solid line) and $TC_{16}PyP(4)$/anthraquinone (1 : 1) mixed monolayer (dashed line).

molecular area of Mn(III)TPP(CO_2H) decreased with the incorporation of *n*-hexadecane.

3.2 LAXD of $TC_{16}PyP(4)$ LB films and $TC_{16}PyP(4)$/AnQ mixed LB films

Fig. 4 and 5 show the LAXD patterns of pure $TC_{16}PyP(4)$ LB films and $TC_{16}PyP(4)$/AnQ mixed LB films, respectively. There is a well defined Bragg diffraction peak at 2.20° for pure $TC_{16}PyP(4)$ LB films and at 2.01° for $TC_{16}PyP(4)$/AnQ mixed LB films, which corresponds to the (001) Bragg peak. In addition relatively weak subsidiary peaks were observed at angles below the (001) Bragg peak. The number of subsidiary diffraction peaks η can be predicted by the relation $\eta=(N/2)-2$ (N=number of unit cells).[17] These results show that both $TC_{16}PyP$ LB films and $TC_{16}PyP(4)$/AnQ mixed LB films show good interlayer order. According to Bragg's formula: $n\lambda=2d\sin\theta$, the value of d is 4.05 nm for $TC_{16}PyP(4)$ and 4.26 nm for 1 : 1 $TC_{16}PyP(4)$/AnQ. For Y-mode LB films, $d/2$ is equal to the monolayer thickness. Therefore, the monolayer thickness of $TC_{16}PyP(4)$ LB films and $TC_{16}PyP(4)$/AnQ mixed LB films is 2.03 and 2.13 nm, respectively, *i.e.*, the monolayer thickness of the $TC_{16}PyP(4)$/AnQ mixed LB film is slightly larger than that of the pure $TC_{16}PyP(4)$ LB film. This fact may be explained by hydrophobic interactions of the long hydrocarbon chains being intensified in the mixed monolayer. As a result, the long chains of $TC_{16}PyP(4)$ in the mixed LB films are slightly more extended than in the pure $TC_{16}PyP(4)$ monolayer. This result is similar to that found in the literature for related systems.[15]

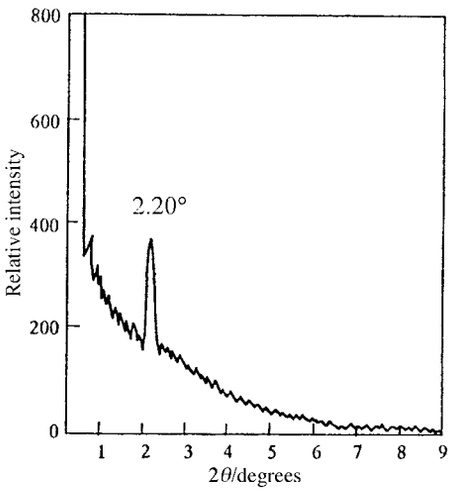

Fig. 4 LAXD patterns of a pure $TC_{16}PyP(4)$ LB film (39 monolayers).

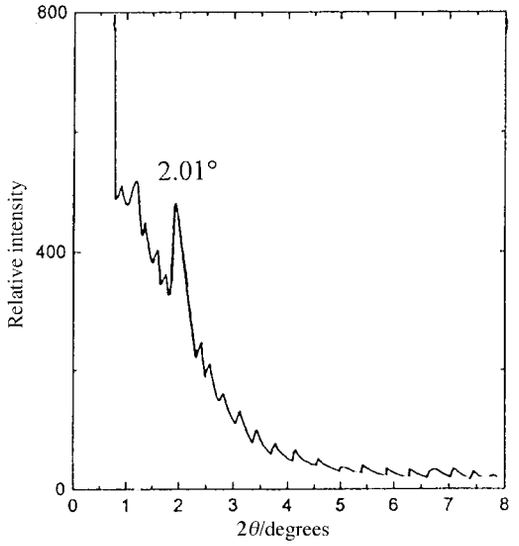

Fig. 5 LAXD patterns of a $TC_{16}PyP(4)$/AnQ mixed LB film (39 monolayers).

$TC_{16}PyP(4)$ is a typical amphiphilic molecule with four hydrocarbon chains extending to the air phase and the porphyrin ring nearly lying flat on the air/water interface in the monolayer, *i.e.* resembling a cylinder with a large cavity. The anthraquinone molecule is hydrophobic, so that when the mixed $TC_{16}PyP(4)$/AnQ monolayer is compressed, anthraquinone molecules will be incorporated into the cavity of the cylindrical porphyrin molecule. We infer that the anthraquinone molecules are arranged in the cavity within the long chains of $TC_{16}PyP(4)$ in monolayers of the mixed LB films.

3.3 UV–VIS spectra of $TC_{16}PyP(4)$ LB films and $TC_{16}PyP(4)$/AnQ mixed LB films

Fig. 6 compares the absorption spectra of the 1 : 1 $TC_{16}PyP(4)$/AnQ mixed LB film (solid line) with that of a 1 : 1 $TC_{16}PyP(4)$/AnQ mixed solution (dashed line). The absorption spectra of the 1 : 1 $TC_{16}PyP(4)$/AnQ mixed solution is nearly identical to the sum of the spectra of the pure porphyrin and AnQ, indicating that there are no strong interactions between the two chromophores in the ground state. For the 1 : 1 $TC_{16}PyP(4)$/AnQ mixed LB film, the absorption bands of $TC_{16}PyP(4)$ and AnQ are red-shifted relative to those in solution with concomitant broadening of $\Delta\nu_{1/2}$ (width at half height). These changes are attributed to the incorporation of AnQ molecules and close intermolecular contacts between $TC_{16}PyP(4)$ and AnQ, resulting in overlap of the large π bands of $TC_{16}PyP(4)$ and AnQ. This leads to an intermolecular transition energy decrease and the absorption bands are thus red-shifted.[18]

The absorption bands of $TC_{16}PyP(4)$ in the mixed LB films are slightly blue-shifted (*ca.* 2–5 nm) relative to those of $TC_{16}PyP(4)$ in pure $TC_{16}PyP(4)$ LB films. AnQ molecules can accept electrons while the porphyrin ring can act as an electron donor. It is possible that interactions between the anthraquinone and porphyrin occur when anthraquinone molecules are incorporated into the porphyrin cavity, as in calixarene/C_{60}[19] and poly(*N*-vinylcarbazole)/C_{60} mixed systems.[20] Such interactions may make it more difficult for the porphyrin to form aggregates. Because the absorptions of porphyrins are mainly determined by their aggregation state, we observe that the absorption bands of $TC_{16}PyP(4)$ in mixed LB films are slightly blue-shifted relative to that for the pure porphyrin film. These observations also support the inference that anthraquinone molecules are incorporated into the cavity of $TC_{16}PyP(4)$ in the $TC_{16}PyP(4)$/AnQ mixed LB films.

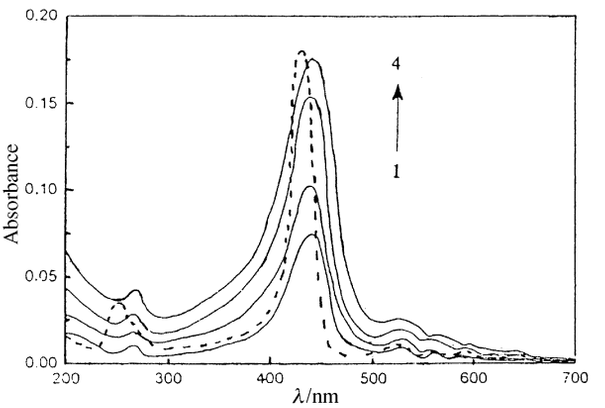

Fig. 6 UV–VIS absorption spectra of a mixture of $TC_{16}PyP(4)$ and AnQ in $CHCl_3$ and LB films [$CHCl_3$ solution (dashed line), LB films (solid lines): 1→4, 6, 14, 26 and 38 monolayers].

Measurement of the absorbance at 263 nm (C) and 433 nm (B) in the UV–VIS spectra of 1 : 1 $TC_{16}PyP(4)$/AnQ mixed LB films *vs.* the number of layers results in a straight line (Fig. 7), and indicates that the $TC_{16}PyP(4)$/AnQ mixed monolayers at the air/water interface are well transferred onto the substrate and that the microscopic environment of the porphyrin and $TC_{16}PyP(4)$/AnQ remains unchanged with layer number.

3.4 Photoelectric properties of $TC_{16}PyP(4)$/AnQ mixed LB films

Photocurrent–time response curves of $TC_{16}PyP(4)$/AnQ mixed LB films (three layers) are shown in Fig. 8. Fig. 8(a) shows the photocurrent–time response curve of SnO_2 OTE itself. Owing to the use of a 390-nm cut-off filter, the blank photocurrent of SnO_2 OTE is almost zero and so interference of the SnO_2 OTE can be disregarded. Fig. 8(b) shows the photocurrent–time response curve of $TC_{16}PyP(4)$/AnQ mixed LB films, in an electrolyte solution of aqueous 0.1 mol L^{-1} KCl. As can be seen, the photocurrent shows a rapid rise and reached a maximum value of *ca.* 40 nA cm^{-2} once the light was turned on, followed by an exponential decrease and reaching a steady value of *ca.* 20 nA cm^{-2} several seconds later. Turning off the light, the photocurrent rapidly declined to zero. Such a behaviour has been reported for a chlorophyll layer deposited on an SnO_2 OTE.[14] During the first stage of irradiation, because there is an inadequate supply of electrons by a donor to $TC_{16}PyP(4)$*, partial oxidative decomposition of $TC_{16}PyP(4)$ may possibly occur following electron injection to SnO_2. Then, the photocurrent shows a decay; as a result of movement of donors in the electrolyte solution, there will be an equilibrium between the number of electrons injected to SnO_2 from $TC_{16}PyP(4)$* and the number of electrons abstracted from a donor, which leads to a dynamic equilibrium level of $TC_{16}PyP(4)$* molecules in the LB films so leading to a levelling off of the photocurrent.

When electron donating ascorbic acid (80 mmol L^{-1}) was added to the 0.1 mol L^{-1} KCl electrolyte solution, the maximum and steady photocurrent were increased to 250 and 100 nA cm^{-2}, respectively [Fig. 8(c)]. Fig. 8(d) shows the photocurrent–time response of $TC_{16}PyP(4)$/AnQ LB films in the presence of the acceptor *p*-benzoquinone (1 mmol L^{-1}) in the 0.1 mol L^{-1} KCl electrolyte solution. With the addition of the electron acceptor, the maximum and steady photocurrent were increased to −580 and −420 nA cm^{-2}, respectively. Clearly, however, the direction of photocurrent is reversed.

Fig. 9 shows the photovoltage–time response curves of $TC_{16}PyP(4)$/AnQ LB films. Fig. 9(a) shows the photovoltage—time response curve of $TC_{16}PyP(4)$/AnQ LB films (three layers) in an electrolyte solution of aqueous 0.1 mol L^{-1} KCl containing 80 mmol L^{-1} ascorbic acid. The photovoltage rapidly reached a maximum value of 50 mV once the sample was irradiated and during illumination, the photovoltage remained constant. Turning off the light, the photovoltage showed slow exponential decay. When the electrolyte solution was changed to 0.1 mol L^{-1} KCl aqueous solution containing 1 mmol L^{-1} *p*-benzoquinone, the photovoltage–time response curve of $TC_{16}PyP(4)$/AnQ LB films is as in Fig. 9(b). The photovoltage was −80 mV at the commencement of irradiation and remained constant during the illumination. Turning off the light, the photovoltage also showed slow exponential decay. It is remarkable that there is an obvious difference in the decay characteristics of the photocurrent and photovoltage and similar phenomena have been observed in the photovoltage of an R-phycoerythrin/SnO_2 OTE electrochemical cell.[21] At present, the cause of this difference is unclear and further careful investigations will be necessary.

In a previous study[7] we suggested that the photoelectric response of $TC_{16}PyP(4)$ LB films is a result of a photo-induced charge transfer mechanism. The photocurrent increases in the presence of electron donor were attributed to supersensitization. Such a mechanism and interpretation may also be applicable to the photoelectric response of $TC_{16}PyP(4)$/AnQ mixed LB films. Here, we emphasise the consequences of the effect of incorporation of AnQ into the cavity of $TC_{16}PyP(4)$ on the photovoltaic effect of $TC_{16}PyP(4)$ LB films and quantitative data on the photocurrent and photovoltage of the two photocells, $TC_{16}PyP(4)$ and $TC_{16}PyP(4)$/AnQ are summarized in Tables 1 and 2, respectively.

Examination of the data shows that under identical conditions, the direction of the photocurrent and photovoltage of the two photocells is identical and the variations of the

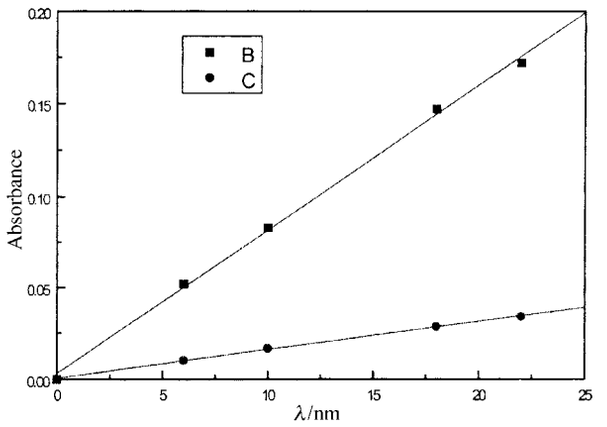

Fig. 7 Dependence of absorbance at 263 nm (C) and 433 nm (B) for mixed LB films.

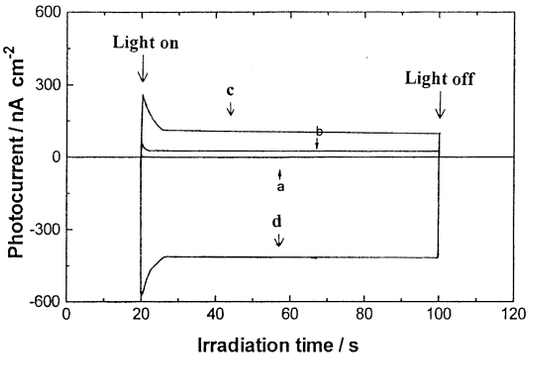

Fig. 8 Photocurrent–time responses of (a) a clean SnO_2 OTE (0.1 M KCl electrolyte solution) and of $TC_{16}PyP(4)$/AnQ LB films (three monolayers), electrolyte solution: (b) 0.1 M KCl, (c) 0.1 M KCl + 80 mM ascorbic acid and (d) 0.1 M KCl + 1 mM *p*-benzoquinone solution. Light source: 500 W xenon arc light (> 390 nm), 80 mW cm^{-2}.

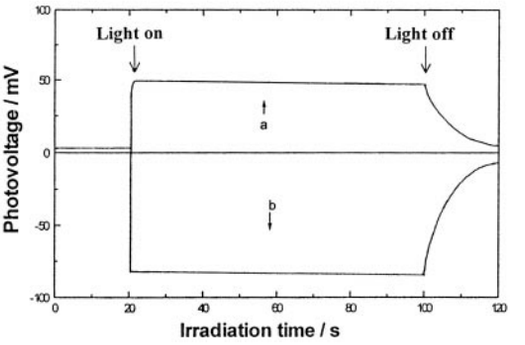

Fig. 9 Photovoltage–time responses of $TC_{16}PyP(4)$/AnQ LB films (three monolayers). Electrolyte composition: (a) 0.1 M KCl + 80 mM ascorbic acid solution; (b) 0.1 M KCl + 1 mM *p*-benzoquinone aqueous solution. Light source: 500 W xenon arc light (> 390 nm), 80 mW cm^{-2}.

Table 1 Photocurrent data[a]

Photocell	0.1 M KCl	0.1 M KCl+80 mM AA[b]	0.1 M KCl+1 mM *p*-benzoquinone
Pure $TC_{16}PyP(4)$ LB film	60–30	400–250	−950 to −800
$TC_{16}PyP(4)$/AnQ LB film	40–20	250–100	−580 to −420

[a]Photocurrent is in nA cm^{-2}. [b]AA = ascorbic acid.

Table 2 Photovoltage data[a]

Photocell	0.1 M KCl+ 80 mM AA[b]	0.1 M KCl+ 1 mM *p*-benzoquinone
Pure $TC_{16}PyP(4)$ LB film	90	−110
$TC_{16}PyP(4)$/AnQ LB film	50	−80

[a]Photocurrent is in mV. [b]AA = ascorbic acid.

photocurrent and photovoltage are similar. However, the values of the photocurrent and photovoltage of $TC_{16}PyP(4)$/AnQ mixed LB films are lower than those observed in the $TC_{16}PyP(4)$ LB films. Such a result can reasonably be rationalized as follows.

The decrease of photocurrent and photovoltage of $TC_{16}PyP(4)$/AnQ mixed LB films relative to those of pure $TC_{16}PyP(4)$ LB films in a 0.1 mol L^{-1} KCl electrolyte solution can be explained by effective removal of the electron from excited $TC_{16}PyP(4)$* by AnQ, so reducing the efficiency and the velocity of electron injection to the conduction band of the SnO_2 electrode.

When an electron donor is added to the 0.1 mol L^{-1} KCl electrolyte solution, two possible pathways are possible leading to a decrease of the photocurrent and photovoltage of $TC_{16}PyP(4)$/AnQ mixed LB films: (i) competitive abstracting of the electron from the electron donor between the cation radical $TC_{16}PyP(4)^{+}$ (resulting from electron injection to the conduction band of the SnO_2 electrode from the excited porphyrin $TC_{16}PyP(4)$*) and AnQ, so reducing the regeneration of the photoactive state $C_{16}PyP(4)$*; (ii) competitive abstracting of the electron from the electron donor between the excited porphyrin $TC_{16}PyP(4)$* and AnQ reducing the production of anion radical $TC_{16}PyP(4)^{-\cdot}$, which has a stronger electron donating ability than $TC_{16}PyP(4)$*, so reducing the efficiency of electron injection to the SnO_2 electrode.

For an electrolyte solution containing the electron acceptor *p*-benzoquinone, both *p*-benzoquinone and AnQ directly capture the electron of the excited $TC_{16}PyP(4)$*, producing the cation radical $TC_{16}PyP(4)^{+\cdot}$, leading to electron injection from the conduction band of SnO_2 to the reduced porphyrin $TC_{16}PyP(4)^{+\cdot}$, resulting in a reversed photocurrent. In addition, AnQ molecules in mixed LB films also extract some conduction electrons injected from $TC_{16}PyP(4)$*, which reduces the efficiency and speed of electron transfer from the conduction band of the SnO_2 electrode to the reduced porphyrin $TC_{16}PyP(4)^{+\cdot}$, so reducing the photocurrent and photovoltage. A detailed mechanism involving these influential factors will be further elaborated by future studies.

Conclusions

A 1:1 $TC_{16}PyP(4)$/anthraquinone mixture can form a stable mixed monolayer at the air/water interface. $TC_{16}PyP(4)$/AnQ mixed monolayers can be transferred to glass, quartz and SnO_2 OTE substrates. Most AnQ molecules are incorporated in the cavities between the long alkyl chains of $TC_{16}PyP(4)$ molecules in a mixed monolayer and in LB films. The porphyrin/AnQ mixed LB film can be regarded as a two-dimensional host–guest system. $TC_{16}PyP(4)$/AnQ LB films have good stability, homogeneous structure and periodicity. The photocurrent and photovoltage of an electrochemical cell of $TC_{16}PyP(4)$/AnQ LB films deposited on SnO_2 OTE are apparently lower than those from a photocell of pure $TC_{16}PyP(4)$ LB films owing to the incorporation of AnQ.

Acknowledgements

This project (59573010) was supported by the Natural Nature Science Foundation of China.

References

1 F. J. Kampas, K. Yamashita and J. Fajer, *Nature*, 1980, **284**, 40.
2 A. Desormeaux, J. J. Max and R. M. Leblanc, *J. Phys. Chem*, 1993, **97**, 6670.
3 V. Y. Merritt and H. J. Hovel, *Appl. Phys. Lett.*, 1976, **29**, 414.
4 A. W. Snow and N. L. Jarvis, *J. Am. Chem. Soc.*, 1984, **106**, 4706.
5 J. C. Shen, X. Zhang and Y. P. Sun, *Prog. Nat. Sci.*, 1997, **7**, 1.
6 Y. Nishikata, A. Morikawa, M. A. Kakimoto, Y. Imai, Y. Hirata, K. Nishiyama and M. Fujihira, *J. Chem. Soc., Chem. Commun.*, 1989, **120**, 1772.
7 X. Z. He, G. M. Xia, Y. L. Zhou, M. H. Zhang and T. Shen, *Sci. China, Ser. B*, 1998, **41**, 633.
8 Y. N. Zhu, X. R. Xiao, H. J. Xu and B. W. Zhang, *Photogr. Sci. Photochem.*, 1992, **10**, 46.
9 A. Osuka, T. Nagata and K. Maruyama, *Chem. Lett.*, 1991, **3**, 481.
10 J. Feitelson and D. C. Mauzerall, *J. Phys. Chem.*, 1993, **97**, 8410.
11 T. Asahi, M. Ohkohchi, R. Matsusaka, N. Mataga, R. P. Zhang, A. Osuka and K. Maruyama, *J. Am. Chem. Soc.*, 1993, **115**, 5665.
12 X. Z. He, Y. L. Zhou, L. X. Wang, T. K. Li, M. H. Zhang and T. Shen, *Spectrochim. Acta, Part A*, 1999, **55**, 823.
13 H. Grüninger, D. Möbius and H. Meyer, *J. Chem. Phys.*, 1983, **79**, 3701.
14 T. Miyasaka, T. Watanabe, A. Fujishima and K. Honda, *J. Am. Chem. Soc.*, 1978, **100**, 6657.
15 W. R. Scheidt, *Acc. Chem. Res.*, 1977, **10**, 339.
16 H. G. Liu, X. S. Feng and K. Z. Yang, *Chin. J. Chem.*, 1995, **13**, 415.
17 M. Pomerantz and A. Segmuller, *Thin Solid Films*, 1980, **68**, 33.
18 S. Y. Luk, F. R. Mayers and J. O. Williams, *Thin Solid Films*, 1988, **157**, 69.
19 R. M. Williams and J. W. Verhoeven, *Recl. Trav. Chim. Pays-Bas*, 1992, **111**, 531.
20 C. C. Wang, B. J. Deng and S. K. Fu, *Chem. J. Chin. Univ.*, 1994, **15**, 1559.
21 J. A. He, L. J. Jiang, Z. C. Bi and L. Jiang, *Sci. China, Ser. B*, 1996, **39**, 390.

Paper a907900i